Original Paper *Forma*, **27**, 55–69, 2012

A Coding-Theoretical Approach to Analyzing Sequential Patterns of the Sixty-Four Hexagrams in the *I Ching*

Kazuya Hayata

Department of Socio-Informatics, Sapporo Gakuin University, Ebetsu 069-8555, Japan
E-mail address: hayata1@hotmail.co.jp

(Received May 10, 2011; Accepted March 16, 2012)

The sequential patterns of the sixty-four hexagrams in the *I Ching* (the Book of Changes) are analyzed by calculating a divergence between adjacent hexagrams. Geometrically, the divergence is equivalent to the Hamming distance between nodes on a six-dimensional hypercube. Detailed comparisons are made between results for the received ordering of the hexagrams and those for other orderings currently available. Emphasis is on the finding that the received order possesses a sophisticated mathematical structure, suggesting at the same time that it would hold great significance as an integral whole of a human archetype.
Key words: City-Block Distance, Hamming Distance, Hypercube, *I Ching* Mandala, Sixty-Four Hexagrams

1. Introduction

In China the teachings of Confucius (551–479 B.C.) have been expounded on the basis of the four books and the five canons termed the Nine Chinese Classics as listed in Appendix A. Among them the *I Ching* (the Book of Changes) is regarded as an implied canon in Confucianism. Although this canonical text originated from a divination teaching, an exceptionally long period ranging over three thousand years has established it as a representative classic implying an archetype of the Chinese philosophy (Honda, 1997). In the *I Ching* there are sixty-four hexagrams called *gua*'s (Fig. 1), which can be obtained through the eight combinations among eight hexagrams (i.e., $8^2 = 64$) being composed with the three symbols of *yin* (divided line) and *yang* (undivided line). In actual divination, instead of the conventional method using bamboo sticks, the method using coins is useful (Kawamura, 1994), where one will toss three identical coins praying what he/she wants to divine; six trials are needed to determine the specific *gua*. Subsequently, fortune-telling will be made on the instructions of sentences attached to each *gua* although they are in general full of connotations. Aside from divination, in recent years, stochastic behavior due to the *yin-yang* dualism of the *I Ching* has found application to unexpected fields such as depth psychology (Progoff, 1973; Bolen, 1979) and musical composition. Indeed, John Cage (1912–1992) started work on the composition of *Music of Changes* by preparing charts of square numbers for tempi, dynamics, sounds or rests, durations and overlapping. Chance, which he consulted by means of tossing coins (the shortened version of the yarrow stalk oracle), decides which of the given materials are to be combined. The result was written down in a comparative manner according to a pattern of previously devised bars so that the sequence was now definitely determined and the individual sound event in every parameter occurred with the greatest possible precision (Henck, 1988). As is shown in Fig. 2, each hexagram possesses the name written with a single or two Chinese characters, which, in addition to a certain role in the highly symbolic system, can be interpreted as a tag for discriminating a *gua* from others. In addition to the unequal division ($64 = 30 + 34$) of hexagrams between the Upper and the Lower Canon, the method of giving a title to hexagrams appears somewhat paradoxical; for instance, the tag 'After Completion' for the 63rd *gua* is placed prior to 'Before Completion' for the last *gua*. However, it is this whimsicality that makes the study on the *I Ching* fascinating. Among 64! permutations of the hexagrams, the one shown in Fig. 2 (Type I) is known as the most received ordering, wherein we can find the following rule for composing the sequence: 1) The sequence must be juxtaposed in pairs as (1, 2), (3, 4), ..., (63, 64), i.e., there arise thirty-two pairs in the entire sequence. 2) Within each individual pairs the subsequent *gua* is generated by reversing upside down the preceding one. For instance, the sixth *gua* (111010) becomes the reverse of the fifth one (010111). 3) If twin *gua*'s in a pair hold symmetries across the center axis, then the subsequent *gua* must be obtained by inverting the polarity (*yin* $= 0$ and *yang* $= 1$) of the preceding one. In the sequence we find that four pairs, (1, 2), (27, 28), (29, 30), and (61, 62), meet this condition. The sequence of the hexagrams seen in Fig. 2 is not the only but *a* result that has been generated according to this algorithm with the initial condition, 111111, being given; it appears that this initial code holds a deep meaning in Chinese metaphysics. However, the present algorithm includes ambiguities since no rule is imposed on the condition across the interfaces between adjacent pairs. Here we note that there exist thirty-one interfaces. Although implications of the present ordering are described in a commentary text in the *I Ching*, the interpretation is far from clear and seems highly strained. To date, great effort has been expended to elucidate a math-

Copyright © Society for Science on Form, Japan.

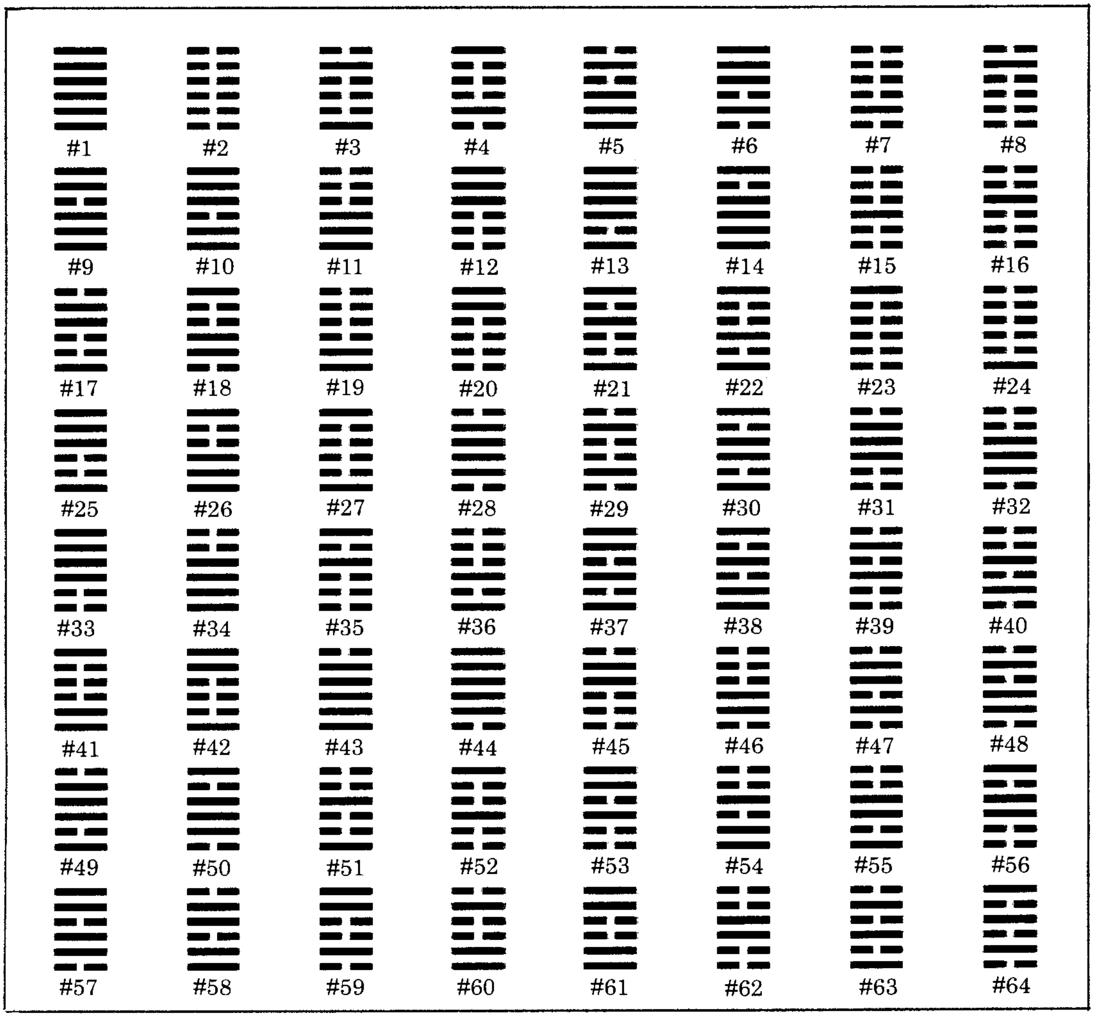

Fig. 1. The sixty-four hexagrams of the *I Ching*. Divided and undivided lines signify, respectively, *yin* and *yang*, which will in what follows be encoded by 0 and 1. The present permutation, termed Type I order in the present paper, obeys the description of *Notes on the Hexagrammatic Order* in the *Ten Wings* of the *I Ching*. The hexagrams that are based upon the *yin-yang* dualism have found unexpected applications. In order to construct a theory of synchronicity, Carl Gustav Jung (1875–1961) performed a divination according to the *I Ching* with shuffling divining sticks for himself (Progoff, 1973; Bolen, 1979). In an experimental attempt to explore the validity of his chance music, John Cage (1912–1992) made compositional decisions with the help of the *I Ching* (Henck, 1988). More recently, it has been mentioned that the underlying concept of the *I Ching* offers a curious resemblance to the encoding scheme of the DNA and protein sequences (Stent, 1969; Yan, 1991; Schonberger, 1992).

ematical meaning of the somewhat whimsical permutation, which, to the author's knowledge, remains unknown (Rutt, 1996; Honda, 1997). In this paper the sequential patterns of the sixty-four hexagrams in the *I Ching* are analyzed by calculating a divergence between adjacent hexagrams (Hayata, 2005). Geometrically, the divergence is equivalent to the Hamming distance between two nodes on a six-dimensional hypercube. In order to explore mathematical implications of the sequential pattern, comparison is made between results for the received ordering of the hexagrams and those for other arrangements. Simultaneously, an attempt is made to map a series of Hamming data onto the two-dimensional space, and eventually to create a prototype of the *I Ching* mandalas.

2. Permutation Patterns of the Sixty-Four Hexagrams

In addition to the received order (Figs. 1 and 2) of the sixty-four hexagrams, there are several methods of ordering, which can be seen in Figs. 3–5. The one shown in Fig. 3 (Type II) is described in *Miscellaneous Notes* [10], which, along with *Notes on the Hexagrammatic Order* [8], constitute the *Ten Wings* being known as ten commentary texts of the *I Ching* (Honda, 1997), where the numerals in the square brackets indicate the order in the *Ten Wings*. Here the Chinese character corresponding to *Wing* implies aiding; although these texts are believed to be edited by Confucius, the truth has not been disclosed. In the *Ten Wings*, in addition to the above two texts, there are eight texts available. It has been recognized that the ordering of Fig. 3, which can be found in *Miscellaneous Notes*, was devised for recital purposes by changing the order of the original sequence (Fig. 2), which can be seen in the main text of the *I Ching*, so that one can learn the canon more easily according to a peculiar rhyming. Note that in Chinese verses the end rhyming becomes an important factor so as to enhance the quality of texts. Indeed such efforts of rhyming would be responsible for making sentences in the last notes a certain miscellany of the explanations of *gua*'s. In com-

(a) 周易上経 (The Upper Canon of the *I Ching*)

1	#1	111111	乾	*Ch'ien/The Creative*
2	#2	000000	坤	*K'un*/The Receptive
3	#3	010001	屯	*Chun*/Difficulty at the Beginning
4	#4	100010	蒙	*Meng*/Youthful Folly
5	#5	010111	需	*Hsu*/Waiting (Nourishment)
6	#6	111010	訟	*Sung*/Conflict
7	#7	000010	師	*Shih*/The Army
8	#8	010000	比	*Pi*/Holding Together
9	#9	110111	小畜	*Hsiao Ch'u*/The Taming Power of the Small
10	#10	111011	履	*Lu*/Treading
11	#11	000111	泰	*T'ai*/Peace
12	#12	111000	否	*P'i*/Standstill
13	#13	111101	同人	*T'ung Jen*/Fellowship with Men
14	#14	101111	大有	*Ta Yu*/Possession in Great Measure
15	#15	000100	謙	*Ch'ien*/Modesty
16	#16	001000	豫	*Yu*/Enthusiasm
17	#17	011001	随	*Sui*/Following
18	#18	100110	蠱	*Ku*/Work on What Has Been Spoiled
19	#19	000011	臨	*Lin*/Approach
20	#20	110000	観	*Kuan*/Contemplation (View)
21	#21	101001	噬嗑	*Shih Ho*/Biting Through
22	#22	100101	賁	*Pi*/Grace
23	#23	100000	剥	*Po*/Splitting Apart
24	#24	000001	復	*Fu*/Return (The Turning Point)
25	#25	111001	无妄	*Wu Wang*/Innocence (The Unexpected)
26	#26	100111	大畜	*Ta Ch'u*/The Taming Power of the Great
27	#27	100001	頤	*I*/The Corners of the Mouth (Providing Nourishment)
28	#28	011110	大過	*Ta Kuo*/Preponderance of the Great
29	#29	010010	坎	*K'an*/The Abysmal (Water)
30	#30	101101	離	*Li*/The Clinging, Fire

Fig. 2. The received (Type I) ordering. The *yin* and *yang* are denoted, respectively, by 0 and 1. Each hexagram possesses the name that is represented with a single or a double Chinese character, which was translated into English by Baynes (Wilhelm, 1968). (a) The Upper Canon of the *I Ching*. (b) The Lower Canon of the *I Ching*.

parison between Figs. 2 and 3 one finds that the replacement is made in pairs. In contrast to those shown in Figs. 1–3, the pairing of hexagrams is broken in the arrangement of Fig. 4 (Type III), which can be seen in the *Mawangdui* manuscript of 168 B.C., the period of the Han dynasty. This manuscript written on a silk sheet was discovered in 1972–1974 by excavating the *Mawangdui* Tomb in Hunan, China. The hexagrams are arranged by octets in each of which all eight have the same upper trigram. The sequence of these upper trigrams takes all the males before all the females, giving the order: father, third son, second son, first son; mother, third daughter, second daughter, first daughter (Rutt, 1996). The three arrangements of hexagrams mentioned above would reflect more or less ancient Chinese philosophy, the profound essence of which seems to be difficult for moderns to understand. For those who have learned the binary logic for use in computer sciences as well as in information theory, the most natural ordering will be the one shown in Fig. 5 (Type IV), which coincides with the six-digit binary counting system that was once studied by Gottfried Wilhelm von Leibniz (1646–1716). Indeed, they say that he was interested in the ancient Chinese thought through communication with the Jesuit missionaries in Peking (Rutt, 1996). In more recent years, similarities have been pointed out between the *I Ching* and the genetic code (Stent, 1969; Yan, 1991; Schonberger, 1992).

3. Analytical Method

3.1 Giving an outline of coding theory

Modern information theory consists of Shannon theory and coding theory. The latter is based on the linear algebra, and therefore, possesses the theoretical system distinctly different from the former that has been developed on the basis of the probability theory as well as statistics. Here we consider a binary sequence of length k, $x_1x_2\dots x_k$, to be transmitted through a communication channel. Subsequently, in order to detect a single error in the sequence, we add a bit, c, to it as

$$\boldsymbol{w} = x_1x_2\dots x_kc, \tag{1}$$

where the original code $x_1x_2\dots x_k$ is termed the information symbol or the information bit, and the additional bit is termed the check symbol (Imai, 1984). For the convenience

(b) 周易下経 (The Lower Canon of the *I Ching*)

31	#31	011100	咸	*Hsien*/Influence (Wooing)
32	#32	001110	恒	*Heng*/Duration
33	#33	111100	遯	*Tun*/Retreat
34	#34	001111	大壮	*Ta Chuang*/The Power of the Great
35	#35	101000	晋	*Chin*/Progress
36	#36	000101	明夷	*Ming I*/Darkening of the Light
37	#37	110101	家人	*Chia Jen*/The Family
38	#38	101011	睽	*K'uei*/Opposition
39	#39	010100	蹇	*Chien*/Obstruction
40	#40	001010	解	*Hsieh*/Deliverance
41	#41	100011	損	*Sun*/Decrease
42	#42	110001	益	*I*/Increase
43	#43	011111	决	*Kuai*/Break-through (Resoluteness)
44	#44	111110	姤	*Kou*/Coming to Meet
45	#45	011000	萃	*Ts'ui*/Gathering Together
46	#46	000110	升	*Sheng*/Pushing Upward
47	#47	011010	困	*K'un*/Oppression (Exhaustion)
48	#48	010110	井	*Ching*/The Well
49	#49	011101	革	*Ko*/Revolution (Molting)
50	#50	101110	鼎	*Ting*/The Caldron
51	#51	001001	震	*Chen*/The Arousing (Shock, Thunder)
52	#52	100100	艮	*Ken*/Keeping Still, Mountain
53	#53	110100	漸	*Chien*/Development (Gradual Progress)
54	#54	001011	帰妹	*Kuei Mei*/The Marrying Maiden
55	#55	001101	豊	*Feng*/Abundance
56	#56	101100	旅	*Lu*/The Wanderer
57	#57	110110	巽	*Sun*/The Gentle (The Penetrating, Wind)
58	#58	011011	兌	*Tui*/The Joyous, Lake
59	#59	110010	渙	*Huan*/Dispersion
60	#60	010011	節	*Chieh*/Limitation
61	#61	110011	中孚	*Chung Fu*/Inner Truth
62	#62	001100	小過	*Hsiao Kuo*/Preponderance of the Small
63	#63	010101	既済	*Chi Chi*/After Completion
64	#64	101010	未済	*Wei Chi*/Before Completion

Fig. 2. (continued).

of the algebra, Eq. (1) will frequently be rewritten in the form of the $(k+1)$-dimensional vector

$$\boldsymbol{w} = (x_1, x_2, \ldots, x_k, c). \tag{2}$$

The main concern in the conventional coding theory lies in finding a specific system of the entire symbols capable of detecting errors. The concept of distances between two vectors and their geometrical representations in a $(k+1)$-dimensional hypercube could be a powerful tool for designing a particular coding system.

3.2 Hamming distance

As a distance between the two n-dimensional binary vectors $\boldsymbol{u} = (u_1, u_2, \ldots, u_n)$ and $\boldsymbol{v} = (v_1, v_2, \ldots, v_n)$ we define

$$d_H(\boldsymbol{u}, \boldsymbol{v}) = \sum_{i=1}^{n} \delta(u_i, v_i) \tag{3}$$

with

$$\delta(u_i, v_i) = \begin{cases} 0 & \text{for } u_i = v_i, \\ 1 & \text{for } u_i \neq v_i. \end{cases} \tag{4}$$

Here one finds that $d_H(\boldsymbol{u}, \boldsymbol{v})$ coincides with the number of unequal pairs in all possible combinations (u_i, v_i) for $i = 1, 2, \ldots, n$. The distance defined with Eq. (3) is termed Hamming distance (Imai, 1984), which is useful for an analytical tool in coding theory. For instance, for $\boldsymbol{u} = (0, 0, 1, 0, 1, 0)$ and $\boldsymbol{v} = (1, 0, 0, 0, 1, 1)$, one obtains $d_H(\boldsymbol{u}, \boldsymbol{v}) = 3$. The Hamming distance meets the so-called three axioms of distance. Specifically

(i) $d_H(\boldsymbol{v}_1, \boldsymbol{v}_2) \geq 0$ (the equality holds for $\boldsymbol{v}_1 = \boldsymbol{v}_2$)
(ii) $d_H(\boldsymbol{v}_1, \boldsymbol{v}_2) = d_H(\boldsymbol{v}_2, \boldsymbol{v}_1)$
(iii) $d_H(\boldsymbol{v}_1, \boldsymbol{v}_2) + d_H(\boldsymbol{v}_2, \boldsymbol{v}_3) \geq d_H(\boldsymbol{v}_1, \boldsymbol{v}_3)$ (the triangular inequality)

where $\boldsymbol{v}_1$, $\boldsymbol{v}_2$, and $\boldsymbol{v}_3$ represent arbitrary n-dimensional binary vectors. Geometrically the distance $d_H(\boldsymbol{u}, \boldsymbol{v})$ is equal

「雑卦伝」排列方式 (The Ordering Scheme in *Miscellaneous Notes*)

1	#1	111111	17	#15	000100	33	#59	110010	49	#55	001101
2	#2	000000	18	#16	001000	34	#60	010011	50	#56	101100
3	#8	010000	19	#21	101001	35	#40	001010	51	#30	101101
4	#7	000010	20	#22	100101	36	#39	010100	52	#29	010010
5	#19	000011	21	#58	011011	37	#38	101011	53	#9	110111
6	#20	110000	22	#57	110110	38	#37	110101	54	#10	111011
7	#3	010001	23	#17	011001	39	#12	111000	55	#5	010111
8	#4	100010	24	#18	100110	40	#11	000111	56	#6	111010
9	#51	001001	25	#23	100000	41	#34	001111	57	#28	011110
10	#52	100100	26	#24	000001	42	#33	111100	58	#27	100001
11	#41	100011	27	#35	101000	43	#14	101111	59	#63	010101
12	#42	110001	28	#36	000101	44	#13	111101	60	#64	101010
13	#26	100111	29	#48	010110	45	#49	011101	61	#54	001011
14	#25	111001	30	#47	011010	46	#50	101110	62	#53	110100
15	#45	011000	31	#31	011100	47	#62	001100	63	#44	111110
16	#46	000110	32	#32	001110	48	#61	110011	64	#43	011111

Fig. 3. The ordering described in *Miscellaneous Notes* in the *Ten Wings* of the *I Ching*, which is termed Type II order in the present paper. The meanings of 0 and 1 are the same as in Fig. 2.

「帛書周易」排列方式 (The *Mawangdui* Order)

1	#1	111111	17	#29	010010	33	#2	000000	49	#30	101101
2	#12	111000	18	#5	010111	34	#11	000111	50	#14	101111
3	#33	111100	19	#8	010000	35	#15	000100	51	#35	101000
4	#10	111011	20	#39	010100	36	#19	000011	52	#56	101100
5	#6	111010	21	#60	010011	37	#7	000010	53	#38	101011
6	#13	111101	22	#63	010101	38	#36	000101	54	#64	101010
7	#25	111001	23	#3	010001	39	#24	000001	55	#21	101001
8	#44	111110	24	#48	010110	40	#46	000110	56	#50	101110
9	#52	100100	25	#51	001001	41	#58	011011	57	#57	110110
10	#26	100111	26	#34	001111	42	#43	011111	58	#9	110111
11	#23	100000	27	#16	001000	43	#45	011000	59	#20	110000
12	#41	100011	28	#62	001100	44	#31	011100	60	#53	110100
13	#4	100010	29	#54	001011	45	#47	011010	61	#61	110011
14	#22	100101	30	#40	001010	46	#49	011101	62	#59	110010
15	#27	100001	31	#55	001101	47	#17	011001	63	#37	110101
16	#18	100110	32	#32	001110	48	#28	011110	64	#42	110001

Fig. 4. The *Mawangdui* order (Type III). The meanings of 0 and 1 are as in Fig. 2.

伏義排列方式 (The *Fuxi* Order Based on the Binary Counting System)

1	#2	000000	17	#8	010000	33	#23	100000	49	#20	110000
2	#24	000001	18	#3	010001	34	#27	100001	50	#42	110001
3	#7	000010	19	#29	010010	35	#4	100010	51	#59	110010
4	#19	000011	20	#60	010011	36	#41	100011	52	#61	110011
5	#15	000100	21	#39	010100	37	#52	100100	53	#53	110100
6	#36	000101	22	#63	010101	38	#22	100101	54	#37	110101
7	#46	000110	23	#48	010110	39	#18	100110	55	#57	110110
8	#11	000111	24	#5	010111	40	#26	100111	56	#9	110111
9	#16	001000	25	#45	011000	41	#35	101000	57	#12	111000
10	#51	001001	26	#17	011001	42	#21	101001	58	#25	111001
11	#40	001010	27	#47	011010	43	#64	101010	59	#6	111010
12	#54	001011	28	#58	011011	44	#38	101011	60	#10	111011
13	#62	001100	29	#31	011100	45	#56	101100	61	#33	111100
14	#55	001101	30	#49	011101	46	#30	101101	62	#13	111101
15	#32	001110	31	#28	011110	47	#50	101110	63	#44	111110
16	#34	001111	32	#43	011111	48	#14	101111	64	#1	111111

Fig. 5. The *Fuxi* order based on the binary counting system (Type IV). The meanings of 0 and 1 are as in Fig. 2.

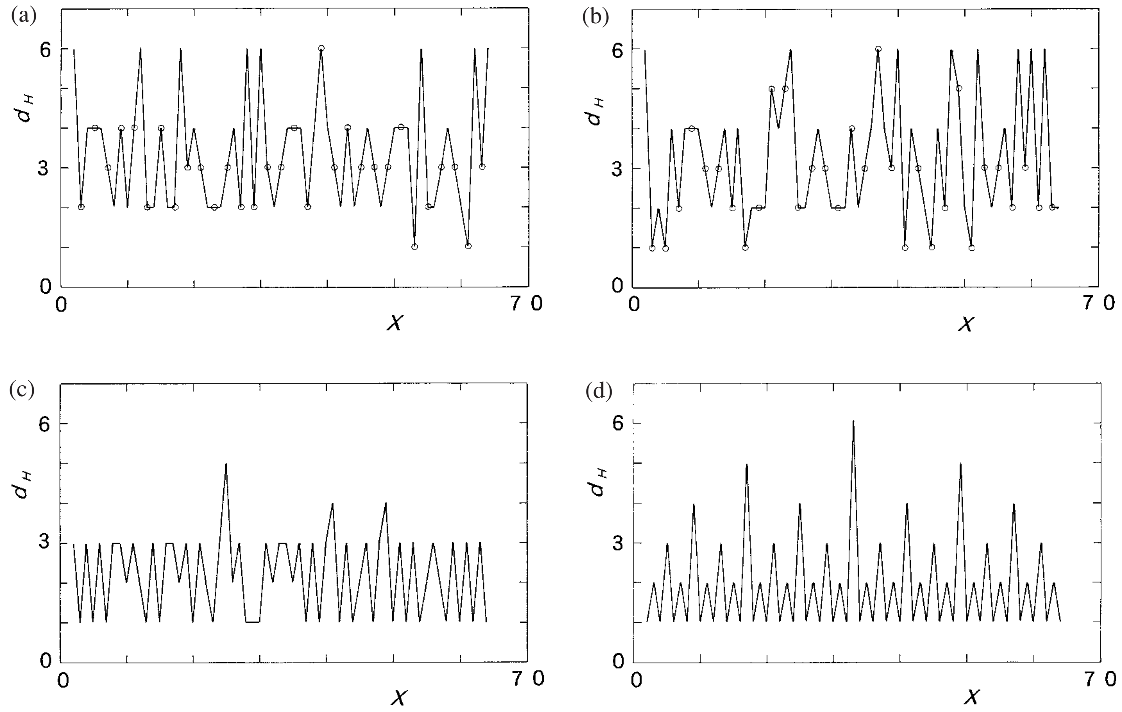

Fig. 6. Variation of Hamming distance, d_H, along the hexagrammatic sequence, x. (a) Received (Type I) order. (b) *Miscellaneous* (Type II) order. (c) *Mawangdui* (Type III) order. (d) *Fuxi* (Type IV) order. In (a) and (b) the hollow circles indicate the distances at the boundaries between adjacent pairs of hexagrams.

to the entire path length between the two position vectors $\boldsymbol{u} = (u_1, u_2, \ldots, u_n)$ and $\boldsymbol{v} = (v_1, v_2, \ldots, v_n)$, provided that the path is restricted solely on the sides of the n-dimensional unit hypercube. In this paper we define the divergence as the Hamming distance between two nodes on the hypercube.

3.3 The city-block (the Manhattan) distance

The concept of the Hamming distance defined for the binary counting system can be extended to the arbitrary n-dimensional Cartesian coordinate as

$$D_1(\boldsymbol{u}, \boldsymbol{v}) = \sum_{i=1}^{n} |u_i - v_i|, \tag{5}$$

where u_i and v_i $(i = 1, 2, \ldots, n)$ are arbitrary real numbers, and the suffix 1 indicates the Minkowski's parameter. In analogy with typical two-dimensional urban systems the distance defined with Eq. (5) is identified frequently with the city-block or, more specifically, the Manhattan distance between the two points in the n-dimensional Euclidean space (Takeuchi, 1989; Jurafsky and Martin, 2009). With the path being restricted along the sides of the n-dimensional hyper rectangular solid, the geometrical interpretation of the present distance is basically identical to the one given for the Hamming system.

4. Results and Discussion

4.1 Comparison between Hamming patterns

The sequential patterns of the Hamming distances between adjacent hexagrams are plotted in Fig. 6 (Hayata, 2005). In comparison among the four patterns for Type I–IV, one can see a variation of its own, which depends sensitively upon the permutation of hexagrams. Among the pat-

Table 1. Comparison among frequency distributions of Hamming distances in Fig. 6.

Distance	Frequency			
	Type I	Type II	Type III	Type IV
1	2	6	22	32
2	20	21	10	16
3	13	10	28	8
4	19	14	2	4
5	0	3	1	2
6	9	9	0	1
Sum	63	63	63	63

Table 2. Comparison among characteristic values of Hamming data in Table 1, where *SD*, *CV*, and μ_3, respectively, stand for the standard deviation, the coefficient of variation, and the third-order moment around the mean.

	Type I		Type II		Type III		Type IV
Σd_H	211	>	203	>	139	>	120
Mean	3.35	>	3.22	>	2.21	>	1.90
Mode	2		2		3		1
Range	5		5		4		5
SD	1.38		1.54		1.01		1.19
CV	0.41		0.48		0.46		0.63
μ_3	1.54		1.78		0.14		2.41

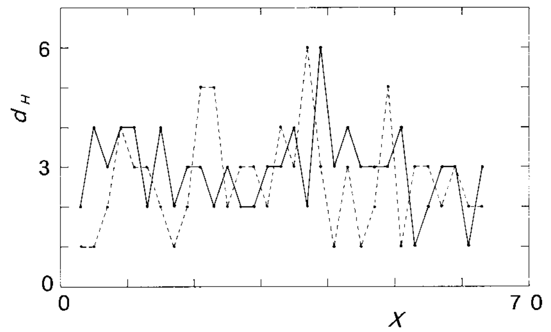

Fig. 7. Variation of Hamming distances on the boundary between pairs of hexagrams. The solid (dashed) lines represent the result for Type I (Type II) order.

Table 3. Comparison between frequency distributions of Hamming data in Fig. 7.

Distance	Frequency	
	Type I	Type II
1	2	6
2	8	9
3	13	10
4	7	2
5	0	3
6	1	1
Sum	31	31

Table 4. Comparison between characteristic values of Hamming data in Table 3.

	Type I	Type II
$\sum d_H$	91	83
Mean	2.94	2.68
Mode	3	3
Range	5	5
SD	1.01	1.30
CV	0.35	0.49
μ_3	0.52	1.55

terns the one for Type II (Fig. 6(b)) exhibits the most complicated behavior, in sharp contrast to the perfect regularity for Type IV (Fig. 6(d)); the other two (Figs. 6(a) and (c)) are found to be intermediate between these extremes. First, we find that the pattern for Type III (Fig. 6(c)) bears some resemblance to the one for Type IV (Fig. 6(d)). However, because of the imperfect periodicity in the former, which is evident for instance from the three exceptional data (the maximum values) at $x = 25, 41$, and 49 in Fig. 6(c), one could conclude that such a resemblance would be incidental and is of no mathematical significance. In particular, sudden jump at $x = 25$, which might remind us of a mutant, arises from the distance between 010110 and 001001. Through comparison among the four patterns, the one for the received ordering (Type I) would show the most significant variation, where there is a certain golden mean between regularity and complexity. In order to confirm this conjecture, the frequency distributions as well as the characteristic values of the Hamming distances are listed, respectively, in Tables 1 and 2. It is interesting to note that the total distance (i.e., the mean) is found to be largest in Type I order and that in this ordering the relation, $d_H \geq 2$, is maintained for the entire region except two points at $x = 53$ and $x = 61$, from which one could infer that on these sites composers of the present arrangement had thrown up their hands in despair. According to coding theory, this relation ensures that a single error in a binary code is detectable (Imai, 1984). The results for Type I arrangement include other features to be noted. From Table 2 we find that, in contrast to the largest mean, the normalized spreading of distances, which can be measured with a coefficient of variation (*CV*), becomes smallest for Type I, where *CV* is defined by the standard deviation (*SD*) divided by the mean. At the same time, we can see from Table 1 that curiously enough there is no frequency for $d_H = 5$, as if composers of Type I order avoided this value with the greatest circumspection. To discuss the property unique to the received order in more detail, the distances at the boundaries between adjacent pairs of hexagrams are shown in Fig. 7 by extracting from Figs. 6(a) and (b) the points marked with hollow circles. The frequency distributions as well as the characteristic values of the data are given, respectively, in Tables 3 and 4; for Type I order, in addition to the third-order moment, $\mu_3 = 0.52$, in Table 4, as the magnitude of the fourth-order moment around the mean, we evaluate $\mu_4 = 4.24$. With these results we can evaluate the skewness $\alpha_3 = \mu_3/SD^3 = 0.50$ as well as the kurtosis $\alpha_4 = \mu_4/SD^4 = 4.07$, from which one would identify the present distribution as a quasisub-Gaussian profile. Note that for $\alpha_3 = 0$ one identifies the profile as the super-Gaussian, purely Gaussian, and sub-Gaussian, respectively, for $0 < \alpha_4 < 3$, $\alpha_4 = 3$, and $\alpha_4 > 3$. In Fig. 7 we would like to arrest attention to the fact that the path of Type I order (solid line) is confined strongly within $2 \leq d_H \leq 4$. Indeed, throughout the entire path there are only three points that miss the target. In particular, for $x \leq 37$, all the points hit the target, and consequently, are focused into the narrow region. Such a feature cannot be seen in the path of Type II ordering (dashed line). Here we shall make a binomial test ($\alpha = 0.01$) with p being the probability of finding a point in the target (i.e., $2 \leq d_H \leq 4$) as

$$H : p = 1/2, K : p > 1/2, \tag{6}$$

where H and K, respectively, are the null and the alternative hypothesis. The cumulative probability of the frequency can be calculated as follows:

$$p(28 \leq Z \leq 31) = 2.3 \times 10^{-6} < \alpha \quad \text{for Type I ordering,} \tag{7a}$$

$$p(21 \leq Z \leq 31) = 3.5 \times 10^{-2} > \alpha \quad \text{for Type II ordering,} \tag{7b}$$

with

$$p(Z = z) = B(31, 1/2) = {}_{31}C_z/2^{31}, \tag{8}$$

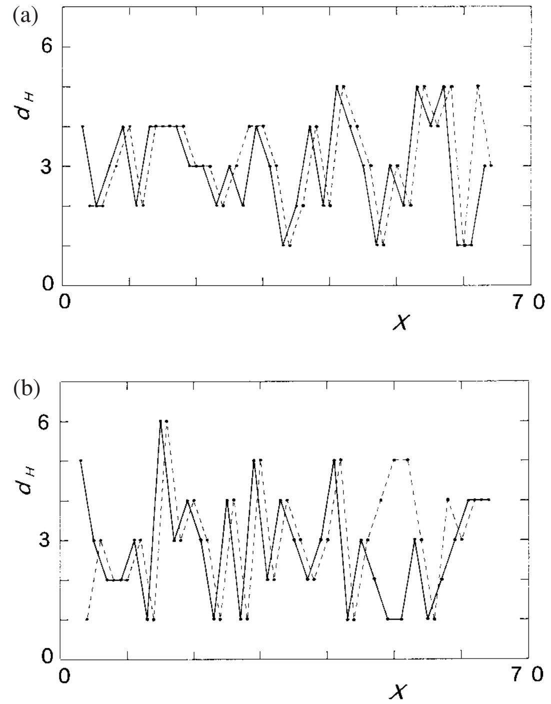

Fig. 8. Variation of Hamming distances between the left or the right side boundaries of adjacent pairs. The solid (dashed) lines indicate the result for the left (right) side boundaries. Incidentally, in (a), the evolutional behavior along the x axis bears only a remote resemblance to a Kármán's vortex in a fluid. (a) Received (Type I) order. (b) *Miscellaneous* (Type II) order.

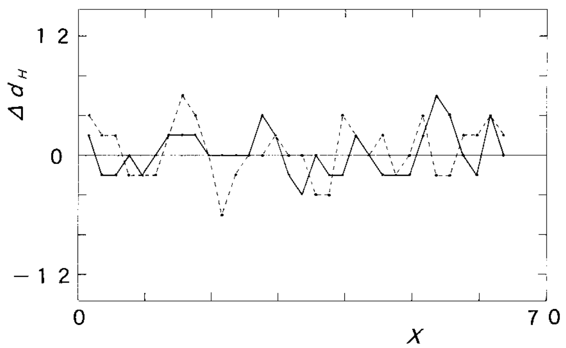

Fig. 9. Stability analysis. Solid lines: Received (Type I) order. Dashed lines: *Miscellaneous* (Type II) order.

where $B(n, p)$ indicates the binomial distribution with its parameters n and p. Therefore H is rejected for Type I ordering, whereas it cannot be rejected for Type II ordering. From the result of the hypothesis test, one could come to the conclusion that composers of the received order carefully determine the arrangement of hexagrammatic pairs so that the orbit does not bounce out from the region as much as possible.

4.2 Hamming distance between pairs

The results for Hamming distances between the left side (solid lines) and the right side (dashed lines) boundaries on neighboring pairs are shown in Fig. 8. Here the arrangement as is illustrated in Fig. 1 (i.e., propagation from left to right) is considered, where the entire system consists of thirty-two pairs $(i, i+1)$ for $i = 1, 3, 5, \ldots, 63$. Note that the neighboring pairs are composed of the head $(i, i+1)$ and the end $(i+2, i+3)$ pairs, where $i = 1, 3, 5, \ldots, 61$. In comparison between the plots of Fig. 8 we notice that the two lines are more synchronous for Type I ordering than for Type II counterpart. Specifically, the city-block distances between the solid and the dashed lines can be evaluated as

$$D_1 = 2 + 2 + 4 = 8 \quad \text{for Type I ordering,} \tag{9a}$$

$$D_1 = 4 + 2 + 4 + 4 + 2 = 16 \quad \text{for Type II ordering,} \tag{9b}$$

indicating that the divergence for the latter becomes two times larger than the one for the former. Again, it appears that the received order (Type I) is of deeper significance than the nonstandard arrangement (Type II).

Table 5. Comparison between frequency distributions of Δd_H's in Fig. 9.

Δd_H	Frequency	
	Type I	Type II
−6	0	1
−4	1	2
−2	10	7
0	10	7
2	7	9
4	3	5
6	1	1
Sum	32	32

Table 6. Comparison between characteristic values of Δd_H's in Table 5.

	Type I		Type II
$\sum \Delta d_H$	8	<	16
Mean	0.25	<	0.50
Mode	−1	<	2
Range	10	<	12
SD	2.28	<	2.74

4.3 Stability analysis

In Fig. 9 the results for a sensitivity test are superimposed with solid (Type I) and dashed (Type II) lines. Here the original arrangement is disturbed by altering the order of hexagrams within a pair. For instance, for the fifth pair, the original order, (9, 10), is reversed as (10, 9), with remaining thirty-one pairs being unperturbed. The ordinate of Fig. 9 stands for the variation of the cumulative Hamming distance, due to the additional perturbation. The frequency distributions as well as the characteristic values, respectively, are compared in Tables 5 and 6. It should be noted herein that, the smaller the magnitudes of the characteristic values become, the more the present arrangement could be regarded as stable. With this criterion we come to the conclusion that, in the presence of the disturbance, Type I arrangement is more stable than Type II counterpart. This conclusion is consistent with those made for Tables 2 and 4.

(a) 「綜卦」排列方式 (A Variant Termed *Zong-gua*)

1	#1	111111	17	#18	100110	33	#34	001111	49	#50	101110
2	#2	000000	18	#17	011001	34	#33	111100	50	#49	011101
3	#4	100010	19	#20	110000	35	#36	000101	51	#52	100100
4	#3	010001	20	#19	000011	36	#35	101000	52	#51	001001
5	#6	111010	21	#22	100101	37	#38	101011	53	#54	001011
6	#5	010111	22	#21	101001	38	#37	110101	54	#53	110100
7	#8	010000	23	#24	000001	39	#40	001010	55	#56	101100
8	#7	000010	24	#23	100000	40	#39	010100	56	#55	001101
9	#10	111011	25	#26	100111	41	#42	110001	57	#58	011011
10	#9	110111	26	#25	111001	42	#41	100011	58	#57	110110
11	#12	111000	27	#27	100001	43	#44	111110	59	#60	010011
12	#11	000111	28	#28	011110	44	#43	011111	60	#59	110010
13	#14	101111	29	#29	010010	45	#46	000110	61	#61	110011
14	#13	111101	30	#30	101101	46	#45	011000	62	#62	001100
15	#16	001000	31	#32	001110	47	#48	010110	63	#64	101010
16	#15	000100	32	#31	011100	48	#47	011010	64	#63	010101

(b) 「錯卦」排列方式 (A Variant Termed *Sagua*)

1	#2	000000	17	#18	100110	33	#19	000011	49	#4	100010
2	#1	111111	18	#17	011001	34	#20	110000	50	#3	010001
3	#50	101110	19	#33	111100	35	#5	010111	51	#57	110110
4	#49	011101	20	#34	001111	36	#6	111010	52	#58	011011
5	#35	101000	21	#48	010110	37	#40	001010	53	#54	001011
6	#36	000101	22	#47	011010	38	#39	010100	54	#53	110100
7	#13	111101	23	#43	011111	39	#38	101011	55	#59	110010
8	#14	101111	24	#44	111110	40	#37	110101	56	#60	010011
9	#16	001000	25	#46	000110	41	#31	011100	57	#51	001001
10	#15	000100	26	#45	011000	42	#32	001110	58	#52	100100
11	#12	111000	27	#28	011110	43	#23	100000	59	#55	001101
12	#11	000111	28	#27	100001	44	#24	000001	60	#56	101100
13	#7	000010	29	#30	101101	45	#26	100111	61	#62	110011
14	#8	010000	30	#29	010010	46	#25	111001	62	#61	001100
15	#10	111011	31	#41	100011	47	#22	100101	63	#64	101010
16	#9	110111	32	#42	110001	48	#21	101001	64	#63	010101

Fig. 10. Altered arrangements for the received (Type I) order. (a) *zong-gua* method. (b) *sagua* method.

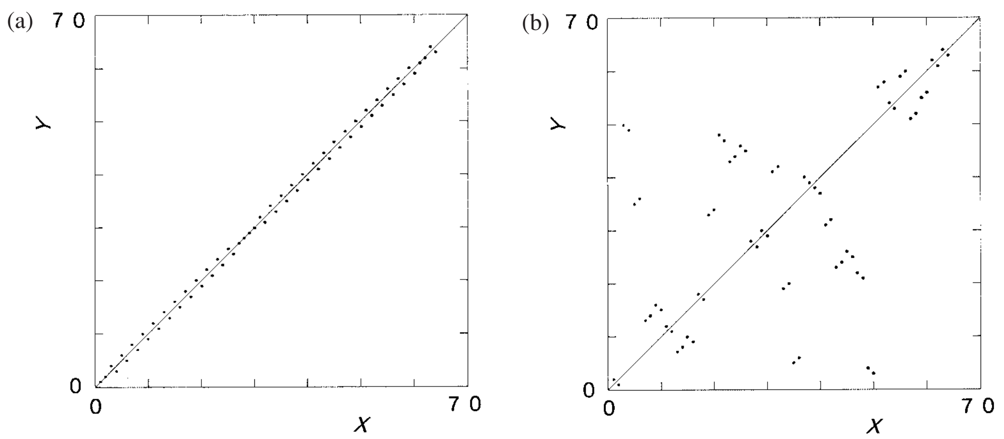

Fig. 11. Scatter diagrams for (a) *zong-gua* ($r_S = 0.999$) and (b) *sagua* ($r_S = 0.549$), where r_S represents the Spearman's rank-correlation coefficient.

4.4 Variants for orderings

There are three methods currently available for obtaining variants of the sequential sixty-four hexagrams, which are termed *zong-gua*, *sagua*, and *wugua* (Kawamura, 1994). As is obvious through comparison between the original sequence, Fig. 2, and its variants that are shown in Figs. 10(a) and (b), *zong-gua* and *sagua*, respectively, are obtainable by turning the original hexagrams upside down and by inverting all the *yin-yang* combinations at once. The scatter diagrams for the two variants (x) are plotted, respectively, in

(a) 「互卦」排列方式 (A Variant Termed *Wugua*)

1	#1	111111	17	#53	110100	33	#44	111110	49	#44	111110
2	#2	000000	18	#54	001011	34	#43	011111	50	#43	011111
3	#23	100000	19	#24	000001	35	#39	010100	51	#39	010100
4	#24	000001	20	#23	100000	36	#40	001010	52	#40	001010
5	#38	101011	21	#39	010100	37	#64	101010	53	#64	101010
6	#37	110101	22	#40	001010	38	#63	010101	54	#63	010101
7	#24	000001	23	#2	000000	39	#64	101010	55	#28	011110
8	#23	100000	24	#2	000000	40	#63	010101	56	#28	011110
9	#38	101011	25	#53	110100	41	#24	000001	57	#38	101011
10	#37	110101	26	#54	001011	42	#23	100000	58	#37	110101
11	#54	001011	27	#2	000000	43	#1	111111	59	#27	100001
12	#53	110100	28	#1	111111	44	#1	111111	60	#27	100001
13	#44	111110	29	#27	100001	45	#53	110100	61	#27	100001
14	#43	011111	30	#28	011110	46	#54	001011	62	#28	011110
15	#40	001010	31	#44	111110	47	#37	110101	63	#64	101010
16	#39	010100	32	#43	011111	48	#38	101011	64	#63	010101

(b) The *Wugua* Ordering of the Sequence in *Miscellaneous Notes*

1	#1	111111	17	#40	001010	33	#27	100001	49	#28	011110
2	#2	000000	18	#39	010100	34	#27	100001	50	#28	011110
3	#23	100000	19	#39	010100	35	#63	010101	51	#28	011110
4	#24	000001	20	#40	001010	36	#64	101010	52	#27	100001
5	#24	000001	21	#37	110101	37	#63	010101	53	#38	101011
6	#23	100000	22	#38	101011	38	#64	101010	54	#37	110101
7	#23	100000	23	#53	110100	39	#53	110100	55	#38	101011
8	#24	000001	24	#54	001011	40	#54	110100	56	#37	110101
9	#39	010100	25	#2	000000	41	#43	011111	57	#1	111111
10	#40	001010	26	#2	000000	42	#44	111110	58	#2	000000
11	#24	000001	27	#39	010100	43	#43	011111	59	#64	101010
12	#23	100000	28	#40	001010	44	#44	111110	60	#63	010101
13	#54	001011	29	#38	101011	45	#44	111110	61	#63	010101
14	#53	110100	30	#37	110101	46	#43	011111	62	#64	101010
15	#53	110100	31	#44	111110	47	#28	011110	63	#1	111111
16	#54	001011	32	#43	011111	48	#27	100001	64	#1	111111

Fig. 12. *Wugua* arrangement for (a) Type I and (b) Type II order. (a) Type I′ order. (b) Type II′ order.

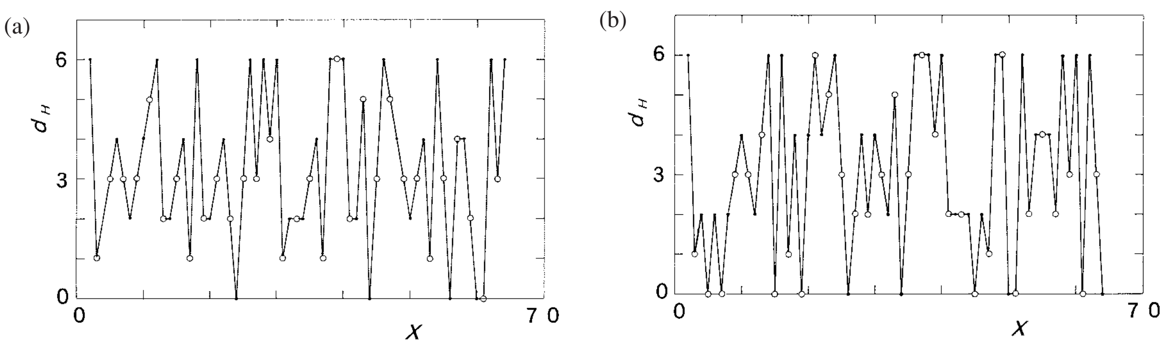

Fig. 13. Variation of Hamming distance, d_H, along the hexagrammatic sequence, x. (a) Type I′ order. (b) Type II′ order. The hollow circles indicate the distances at the boundaries between adjacent pairs of hexagrams.

Figs. 11(a) and (b). In both cases, y indicates Type I order, and symmetry is preserved across the diagonal line $y = x$. Here we note that evidently all the results for the original hexagrams, which have been presented in Figs. 6–9 as well as in Tables 1–6, remain unchanged both for *zong-gua* and for *sagua*. Next, we proceed to the third variant, *wugua*, the definition of which would, in comparison with the other two, be somewhat complicate. To explain the concept of the present variant, we shall rewrite the original hexagram in the symbolic form, $s_1s_2s_3s_4s_5s_6$, with $s_i = 0$ or 1 for $i = 1, 2, \ldots, 6$. With this notation one can generate *wugua* according to the rule (Kawamura, 1994)

$$s_1s_2s_3s_4s_5s_6 \rightarrow s_2s_3s_4s_3s_4s_5. \qquad (10)$$

Table 7. Comparison between frequency distributions of Hamming distances in Fig. 13.

Distance	Frequency	
	Type I′	Type II′
0	5	11
1	5	3
2	14	14
3	13	7
4	10	11
5	3	2
6	13	15
Sum	63	63

Table 8. Comparison between characteristic values of Hamming data in Table 7.

	Type I′	Type II′
$\sum d_H$	205	196
Mean	3.25	3.11
Mode	2	6
Range	6	6
SD	1.84	2.10
CV	0.57	0.68
μ_3	0.51	0.07

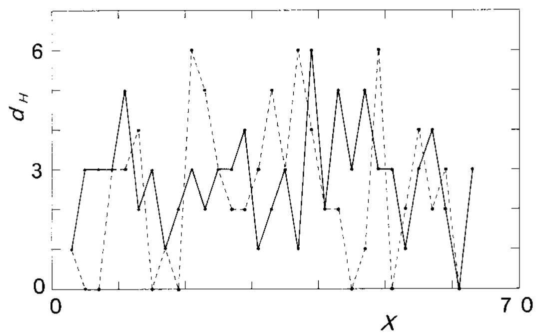

Fig. 14. Variation of Hamming distances on the boundary between pairs of hexagrams. The solid (dashed) lines represent the result for Type I′ (Type II′) order.

Note that with this rule the terminal components, s_1 and s_6, on the original code are removed from the one being altered, and simultaneously the pair s_3s_4 is repeated in it. The *wugua* arrangement that has been realized by Eq. (10) is given in Fig. 12(a), together with the *Miscellaneous* version of the ordering (Fig. 12(b)); the latter corresponds to the arrangement that has been generated by applying Eq. (10) to the one shown in Fig. 3. Applying Eq. (10) to, e.g., the third *gua* in Fig. 3, one obtains

$$010000[\#8] \rightarrow 100000[\#23]$$

with $s_1 = s_3 = s_4 = s_5 = s_6 = 0$, and $s_2 = 1$ being substituted into Eq. (10). In what follows we concentrate on discussing numerical results obtained for Fig. 12.

The variation of the Hamming distance along the hexagrammatic sequence is plotted in Fig. 13(a) for Fig. 12(a) and in Fig. 13(b) for Fig. 12(b), where Type I′ (II′) ordering stands for Type I (II) ordering for *wugua*. In these plots there exist null points where the Hamming distance between neighboring hexagrams vanishes; more nulls can be seen in Fig. 13(b) than in Fig. 13(a). In comparison between Fig. 6 and Fig. 13 the variation of the distance becomes more complicate in Fig. 13, where the distance is fluctuating violently as though it were a white noise. To examine this behavior quantitatively, the frequency distributions as well as the characteristic values of the distances are listed, respectively, in Table 7 and in Table 8. Detailed comparisons between Tables 1 and 7 as well as between Tables 2 and 8 indicate that, in contrast to the decreasing means, the distance data contain more spreading in the *wugua* arrangement, the results of which are indeed consistent with our impression on the comparison between Figs. 6 and 13; the decreasing means would be attributable to the generating null points along the axis of abscissas. The behavior on the boundaries between pairs is highlighted in Fig. 14 by extracting the marked points from Fig. 13, showing, in comparison with Fig. 7, the enhanced complexity along the sequential axis. In particular, for the dashed lines, one can find that the distance is fluctuating with a feature being common to a random walk due to the Brownian motion. This can be confirmed quantitatively in Table 9 and in Table 10, which represent, respectively, the frequency distributions of the Hamming distances and their characteristic values; these should be compared with those listed in Table 3 and in Table 4, respectively. The results for Hamming distances between the boundaries on adjacent pairs are shown in Fig. 15, where the solid (dashed) lines represent the distances between the

Table 9. Comparison between frequency distributions of Hamming data in Fig. 14.

Distance	Frequency	
	Type I′	Type II′
0	1	7
1	5	3
2	6	6
3	13	7
4	2	3
5	3	2
6	1	3
Sum	31	31

Table 10. Comparison between characteristic values of Hamming data in Table 9.

	Type I′	Type II′
$\sum d_H$	85	76
Mean	2.74	2.45
Mode	3	0, 3
Range	6	6
SD	1.34	1.88
CV	0.49	0.77
μ_3	0.77	2.15

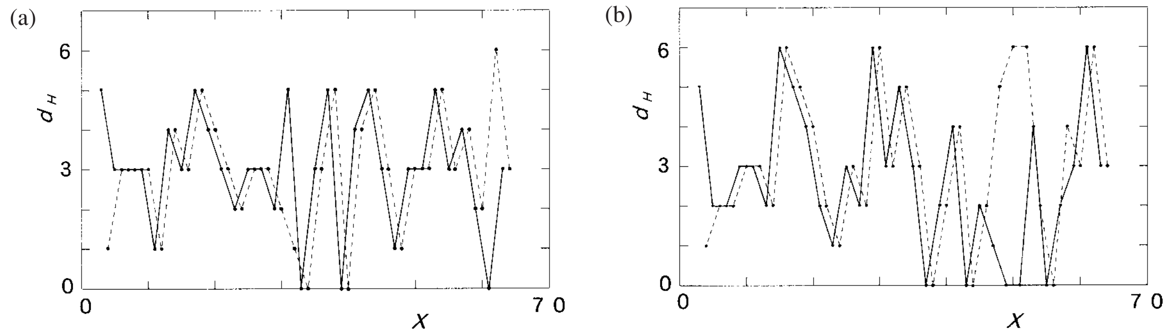

Fig. 15. Variation of Hamming distances between the left or the right side boundaries of adjacent pairs. The solid (dashed) lines indicate the result for the left (right) side boundaries. (a) Type I′ order. (b) Type II′ order.

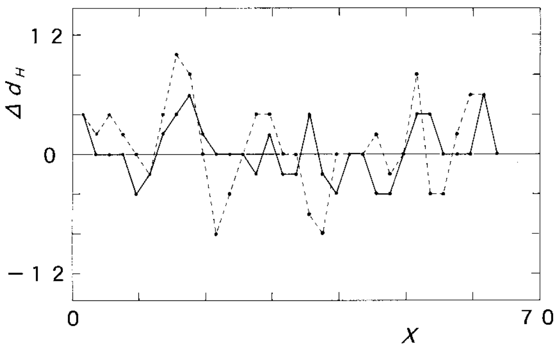

Fig. 16. Stability analysis. Solid lines: Type I′ order. Dashed lines: Type II′ order.

left (right) boundaries, with the arrangement from left to right being considered. In comparison between the plots on Fig. 15 we notice that, although the two lines are more synchronous for Type I′ ordering than for Type II′ counterpart, in both cases the degrees of synchronicity get considerably lower than those observed in Fig. 8. Specifically, the city-block distances between the solid and the dashed lines attain

$$D_1 = 4 + 4 + 6 = 14 \quad \text{for Type I}' \text{ ordering,} \tag{11a}$$

$$D_1 = 4 + 4 + 6 + 6 + 2 + 2 = 24 \quad \text{for Type II}' \text{ ordering.} \tag{11b}$$

These should be compared, respectively, with $D_1 = 8$ (Eq. (9a)) and with $D_1 = 16$ (Eq. (9b)), which have already been given for the original hexagrams. Finally, the results for the stability analysis are superimposed in Fig. 16 with solid (Type I′) and dashed (Type II′) lines, which should be compared with those given in Fig. 9. The frequency distributions as well as the characteristic values, respectively, are listed in Tables 11 and 12. Again, it should be noted that, the smaller is the magnitude of the characteristic values, the more could the present ordering be regarded as stable. With this criterion we come to the conclusion that, in the presence of the disturbance, Type I′ ordering is more stable than Type II′ counterpart. This evaluation coincides with the one that has been made for the analysis of the original hexagrams (Fig. 9) and is consistent with those given for Tables 8 and 10 that have been obtained from the data in Fig. 16.

Table 11. Comparison between frequency distributions of Δd_H's in Fig. 16.

Δd_H	Frequency	
	Type I′	Type II′
−8	0	2
−6	0	1
−4	4	3
−2	5	2
0	13	10
2	3	4
4	5	5
6	2	2
8	0	2
10	0	1
Sum	32	32

Table 12. Comparison between characteristic values of Δd_H's in Table 11.

	Type I′		Type II′
$\sum \Delta d_H$	12	<	28
Mean	0.375	<	0.875
Mode	0	=	0
Range	10	<	18
SD	2.76	<	4.30

4.5 Comparison among city-block distances between Hamming patterns

In summary, quantifying the divergence between Hamming patterns, we shall mention the city-block distances between two patterns being chosen from Figs. 6 and 13. There are fifteen combinations being possible (${}_6C_2 = 15$), the analyzed results of which are given in Table 13, together with the remaining twenty-one ($= 6^2 - 15$) sites being imbedded. As is expectable, aside from six nulls on the diagonal line, one finds that the city-block distance gets minimum for the combinations (Type I, Type I′) and (Type II, Type II′), because Type I′ (II′) is nothing but a variant of Type I (II). In striking contrast to this, it attains the maximum for (Type IV, Type II′), being the distance between the two extremes,

Table 13. Comparison among city-block distances between Hamming patterns shown in Fig. 6 (Type I–IV) and in Fig. 13 (Type I′ and II′).

	TypeI	Type II	Type III	Type IV	Type I′	Type II′
Type I	0	110	104	127	58	127
Type II	110	0	98	123	108	59
Type III	104	98	0	67	124	125
Type IV	127	123	67	0	141	148
Type I′	58	108	124	141	0	127
Type II′	127	59	125	148	127	0

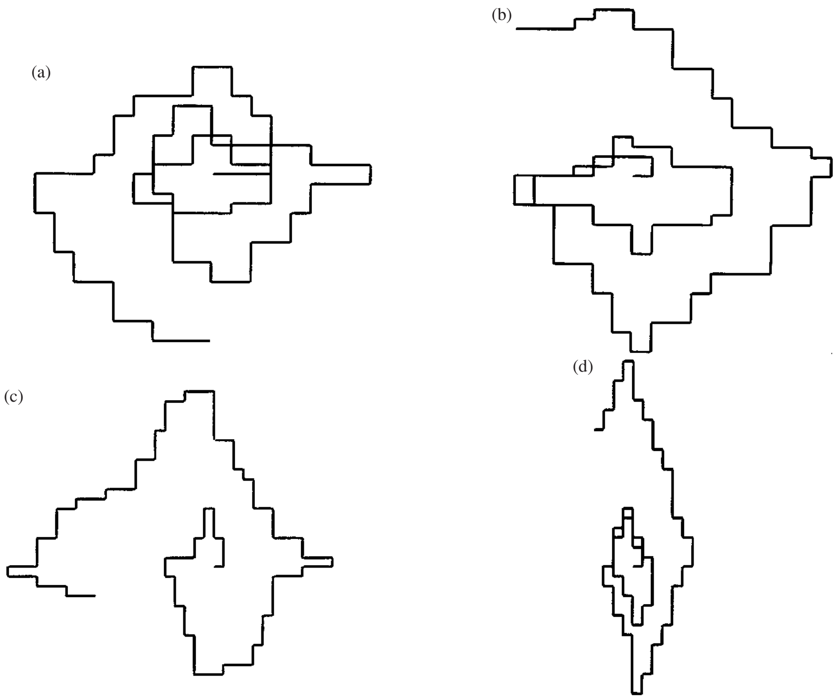

Fig. 17. Two-dimensional expression of a series of Hamming distances with a notched spiral that provides the basis for creating a mandala. (a) Type I order. (b) Type II order. (c) Type III order. (d) Type IV order.

i.e., the most orderly (Fig. 6(d)) and the most chaotic (Fig. 13(b)) variations. A pattern being shifted along the ordinate may possibly shorten the divergence. Actually, shifting Type III pattern upward by unity, we find that $D_1 = 87$ for (Type I, Type III) while $D_1 = 81$ for (Type II, Type III).

5. Creating *I Ching* Mandalas

Mandalas are highly symmetrical arrangements of either geometrical figures (Type A) or sacred symbols (Type B), both of which constellate around the center (Jung, 1968). Originally they were used as means of the religious achievement in the Hinduism as well as the Buddhism. The general interest in the mandalas is nowadays such that they have far exceeded the boundaries of Indology and Tibetology and that the mandalas have now come to be regarded as one of the universal problems directly related to the mysteries of the substructure of the human psyche, as something essential to, and inherent in human nature (Izutsu, 1976). In the course of constructing the system of his depth psychology, which nowadays is known as Jungian psychology, Carl Gustav Jung (1875–1961) appreciated the mandalas as a psychological expression of the totality of the self (Jung, 1968). In the mandalas with its symmetrical arrangement of a variety of archetypal images, one experiences his own inner world as an entirely new, organic, and integral whole. Subsequently, through the study on the *I Ching* and Confucian metaphysics, Toshihiko Izutsu (1914–1993) introduced this concept in his astonishingly comprehensive knowledge of symbolic systems, and aptly expressed it in the term '*I Ching* mandala' (Izutsu, 1976). The *I Ching* mandala signifies the mandalic representation of the sixty-four hexagrams, which are constellated around a center with its configuration preserving the four-fold symmetry. To date, several pictorial representations of the hexagrams, such as the Yellow River Diagram, the Lo River Writing, and illustrations in the form of a magic square, have been categorized into candidates for the *I Ching* mandala. In this section, with application of the spiral mapping technique (Hayata, 2004, 2007) we shall attempt to express in a mandalic form a series of the Hamming data that have been presented in Fig. 6. In this method, from a point on the outermost orbit to the center, a notched spiral with the clockwise rotation is drawn in accordance with the direction of the sequence. However, because of the uncertainty in the location of the

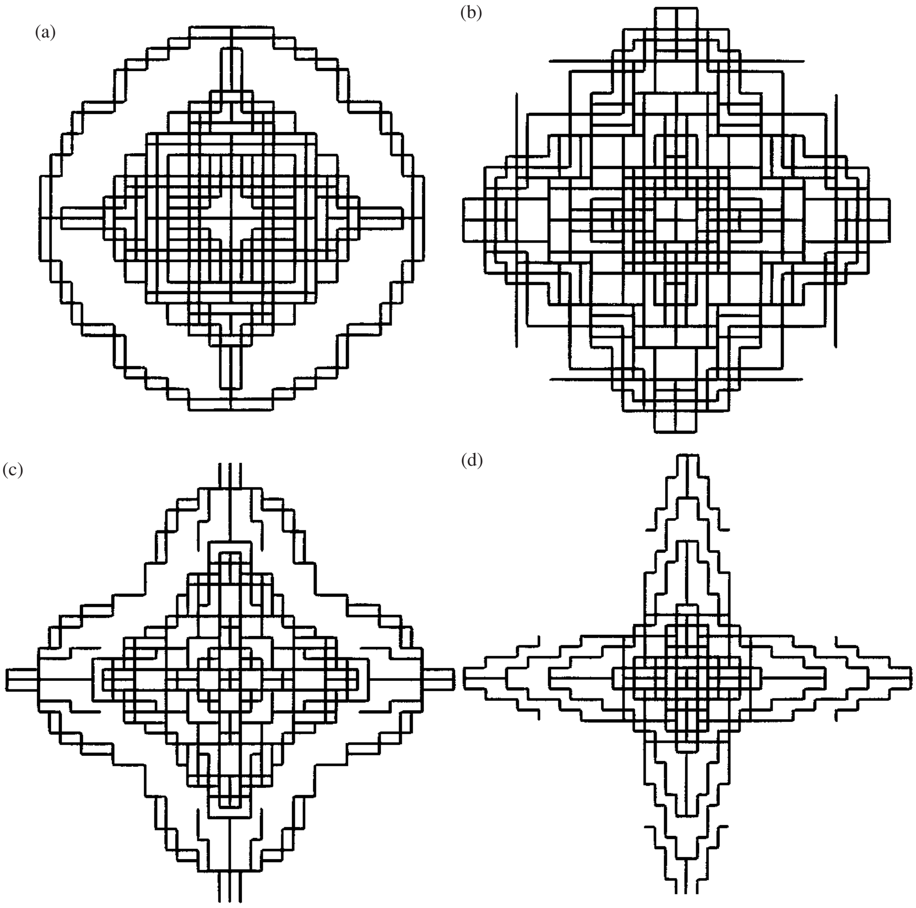

Fig. 18. *I Ching* mandalas realized by the spiral mapping. (a) Type I order. (b) Type II order. (c) Type III order. (d) Type IV order.

initial point, in actual drawings, instead of the forward propagation, a spiral with the counterclockwise rotation is created backward. Applying the spiral mapping technique (see Appendix B) to the sequence of, e.g., Fig. 6(a), one obtains the transition

$$(0,0) \to (6,0) \to (6,1) \to (2,1) \to (2,4) \to (-2,4)$$
$$\to (-2,1) \to (-6,1) \to (-6,-2) \to (-4,-2)$$
$$\to (-4,-4) \to (2,-4) \to (2,-3)$$
$$\to \cdots \to (-6,-15) \to (-6,-17) \to (0,-17).$$

Here the adjacent points are joined with a segment line. The spiral pattern realized with this path is shown in Fig. 17(a), along with the other three, Figs. 17(b)–(d), which have been obtained for the data, respectively, in Figs. 6(b)–(d). Eventually, in order to yield a pattern with the four-fold rotation symmetry, the original pattern and its seven copies are superimposed. The final results are exhibited in Fig. 18, in which a variety of configurations are seen. Among them one would recognize the pattern shown in Fig. 18(b) as most entangled, whereas, in striking contrast to this, the one in Fig. 18(d) exhibits the utmost curiosity with its entire shape being far from the typical mandalic geometry such as a circle and a square. On the other hand, the pattern of Fig. 18(c) would be recognizable as the one considerably akin to an ideal form of mandalas, though its outermost contour dents, which appears to resemble a flower bud waiting for blooming. In pronounced contrast to these three, the drawing of Fig. 18(a), which has been generated from the data of Fig. 6(a), possesses indeed the quality of an authentic mandala as an organic whole, representing a feature in common with a flower being full-blown. In other words, the present pattern could be appreciated as a golden mean between the two extremes (Figs. 18(b) and (d)) mentioned above. Again, we can find an evidence of concluding that the received (Type I) ordering of the sixty-four hexagrams is undoubtedly of most profound significance at least among their permutations currently available.

6. Conclusion

The sequential patterns of the sixty-four hexagrams in the *I Ching* (the Book of Changes) have been analyzed by calculating a divergence between adjacent hexagrams. Geometrically, the divergence is equivalent to the Hamming distance between nodes on a six-dimensional hypercube. Detailed comparisons have been made between the results for the received ordering of the hexagrams and those for other arrangements currently available. Emphasis has been on the finding that the received ordering hides a sophisticated mathematical structure, suggesting at the same time that it would hold great significance as an integral whole of a human archetype. Although the author might simply be playing with a crab on the seashore, he believes that the present paper makes surely a tiny contribution to revealing the secrets of the *I Ching*.

Appendix A. Listing the Four Books (#1 to #4) and the Five Canons (#5 to #9) Which Constitute the Nine Chinese Classics

#1 The Great Disciplines
#2 The Doctrine of the Mean (the Right Path)
#3 The Analects of Confucius
#4 The Discourses of Mencius
#5 The *I Ching* (the Book of Changes)
#6 The *Shu Ching* (the Book of History)
#7 The *Shih Ching* (the Book of Odes)
#8 The *Li Ji* (the Book of Rites)
#9 The *Chunqiu* (the Spring and Autumn Annals)

Appendix B. Outlining the Spiral Mapping Method

1) Start from the center $(0, 0)$ and move horizontally along the x-axis with the increment Δx. Here Δx is the length of the last value of the sequence. For the data of Fig. 6(a), $\Delta x = 6$.

2) Subsequently, move upwards with the increment Δy. Here Δy is the length of the second value from the terminal. For Fig. 6(a), $\Delta y = 1$.

3) For the point being in the first section ($x > 0$, $y > 0$), move backward along the horizontal direction (i.e., set $\Delta x < 0$, being the decrement) and upwards along the vertical direction (set $\Delta y > 0$) until the point attains into the second section ($x < 0$, $y > 0$).

4) For the point being in the second section, move backward along the horizontal direction (set $\Delta x < 0$) and downward along the vertical direction (set $\Delta y < 0$) until the point attains into the third section ($x < 0$, $y < 0$).

5) For the point being in the third section, move forward along the horizontal direction (set $\Delta x > 0$) and downward along the vertical direction (set $\Delta y < 0$) until the point attains into the fourth section ($x > 0$, $y < 0$).

6) For the point being in the fourth section, move forward along the horizontal direction (set $\Delta x > 0$) and upwards along the vertical direction (set $\Delta y > 0$) until the point returns to the first section ($x > 0$, $y > 0$).

7) Return to Step 3 and repeat this procedure until the point attains the initial value of the data.

References

Bolen, J. S. (1979) *The Tao of Psychology*, Harper & Row, San Francisco.

Hayata, K. (2004) Generation of mandala patterns from texts that include sutras, poems and strings of words: method and examples, *Forma*, **19**, 233–264.

Hayata, K. (2005) Pattern dynamics of the sixty-four hexagrams in the *I Ching* and of the eighty-one tetragrams in the *T'ai Hsuan Ching*, *Bulletin of the Society for Science on Form*, **20**, No. 1, 66–67 (in Japanese).

Hayata, K. (2007) Spirally mapped mandalas twilled with Chinese poems, *Forma*, **22**, 247–260.

Henck, H. (1988) *John Cage: Music of Changes*, Wergo, Mainz.

Honda, W. (1997) *The I Ching*, Asahi Newspaper, Tokyo (in Japanese).

Imai, H. (1984) *Information Theory*, Shokodo, Tokyo (in Japanese).

Izutsu, T. (1976) The *I Ching* mandala and Confucian metaphysics, *Eranos Jahrbuch*, **45**, 363–404.

Jung, C. G. (1968) *The Archetypes and the Collective Unconscious* (trans. R. F. C. Hull), 2nd ed., Bollingen Series XX, Princeton University Press, Princeton.

Jurafsky, D. and Martin, J. H. (2009) *Speech and Language Processing*, 2nd ed., Pearson/Prentice Hall, Upper Saddle River, N.J.

Kawamura, M. (1994) *An Introduction to the I Ching*, Mitsumura-Suiko Shoin, Kyoto (in Japanese).

Progoff, I. (1973) *Jung, Synchronicity, and Human Destiny*, Julian, New York.

Rutt, R. (1996) *The Book of Changes (Zhouyi)*, Curzon, Richmond.

Schonberger, M. (1992) *The I Ching & the Genetic Code*, Aurora, Santa Fe.

Stent, G. S. (1969) *The Coming of the Golden Age*, pp. 62–65, Natural History, Doubleday, New York.

Takeuchi, K. (1989) *The Encyclopedia of Statistics*, Toyo Keizai Shimpo, Tokyo, p. 383 (in Japanese).

Wilhelm, R. (1968) *The I Ching or Book of Changes* (trans. C. F. Baynes), 3rd ed., Routledge & Kegan Paul, London.

Yan, J. F. (1991) *DNA and the I Ching*, North Atlantic Books, Berkeley.